Acta Geodyn. Geomater., Vol. 20, No. 4 (212), 155–164, 2023
DOI: 10.13168/AGG.2023.0014
journal homepage: https://www.irsm.cas.cz/acta

ORIGINAL PAPER

MINERALOGICAL, PHYSICOCHEMICAL AND THERMAL INVESTIGATIONS OF TAIBET AND TENDLA SANDS MATERIAL FROM THE NORTHERN ALGERIAN SAHARA

Meriem TOUIL [1], Nassima MEFTAH [2]*, Abderrahim ACHOURI [1], Rachid GHERIANI [3] and Rabiaa BENESSEDIK [1]

[1] *Development of New and Renewable Energies in Arid and Saharan Zones Laboratory, Faculty of Mathematics and Material Sciences, University of Ouargla, 30000 Ouargla, Algeria*
[2] *Department of Physics, Faculty of Exact Sciences, University of El-Oued, El-Oued 39000, Algeria*
[3] *Radiation and Plasma and Surface Physics Laboratory (LRPPS), Faculty of Mathematics and Material Sciences, Department of Physics, University of Ouargla, 30000 Ouargla, Algeria*

**Corresponding author's e-mail:* meftahnassima@yahoo.fr

ARTICLE INFO

Article history:
Received 25 August 2023
Accepted 8 November 2023
Available online 28 November 2023

Keywords:
Dune sand
X-ray diffraction
X-ray fluorescence
Infrared spectroscopy
Quartz
Physicochemical characterization

ABSTRACT

The increasing demand for silicate-based inorganic materials, depleting mineral resources and a growing desertification phenomenon force us to expedite the industrial application of desert sand for environmentally sustainable development. In the present study, the mineralogy, microstructure, phase composition, and thermogravimetric characteristics of Algerian Sahara sand were deeply examined using X-ray diffraction (XRD), Fourier transforms infrared (FTIR), X-ray fluorescence (XRF), Scanning electronic microscope (SEM/EDX) and Thermal analysis (ATG/DTA). The XRD results show that sand samples are very rich in α-quartz with a low content of calcite ($CaCO_3$) and Albite ($NaAlSi_3O_8$), and the quartz crystallite size was in the range of 136-227 nm with high crystallinity. Furthermore, the FTIR, EDX, and XRF analysis demonstrate the dominance of silicon dioxide (90-95 % SiO_2), besides a low ratio of calcium oxide (0.93-3.48 % CaO), and other oxides such as Al_2O_3, and Fe_2O_3. As well as Sahara sand particles were not uniform, which exhibited a variety of morphology and microstructure. ATG/DTA analysis confirms these findings and indicates that this sand was stable at high temperatures. These properties are beneficial in understanding the process and controlling the synthesis and characteristics of the Sahara-sand materials.

1. INTRODUCTION

Silicate compounds are used extensively in a variety of industry applications, including glass, ceramics, road paving, thermal energy storage, building, bridges, and metallurgy. This resulting in massive utilization of minerals including quartz, clay, and aggregates, as well as serious long-term issues of mineral and natural resource consumption in addition to pollution (Shi, 2022; Karnati et al., 2020; Fattouh et al., 2023; Koçak et al., 2020). This emphasizes the need for alternative inactive raw resources such as the river and beach sand, as well as industrial wastes and exhausted quartz sand (Skhvitaridze et al., 2018; Ter et al., 2019; López et al., 2017), whereas the complex nature of their chemical composition causes major challenges in processing stability and product quality. However, sand is a plentiful raw resource in the desert, which covers a wide area of the planet, and their industrial application contributes to both the conservation of nonrenewable natural resources and the prevention of environmental risks. Sand is a loose granular material formed from the disintegration of stones and other materials on the earth's surface (Meftah et al., 2021). Desert sand contains grains ranging in size from 0.0625 to 2 mm with a typical chemical composition of SiO_2 (<90 wt%), Al_2O_3(<16 wt%), and CaO (<20 wt%), Fe_2O_3, MgO, TiO_2, K_2O, and Na_2O. Furthermore, desert sand is one of the most promising materials for producing highly pure quartz (silicon dioxide), amorphous silica, as well as Silicon (Meftah and Hani, 2022; Meftah et al., 2023). Radwan et al. (2021) showed that Arabian desert sands have the potential to be used as a thermal energy storage medium and solar absorber material. Liu et al. (2020) demonstrate that mortar combined with desert sand can be utilized in engineering projects while meeting mortar strength and uniformity criteria and being cost effective. According to another study, coating desert sand with novel hydrophobic and superhydrophobic coatings can be employed for desert water transportation and storage (Atta et al., 2019). Also, El-Mir et al. (2022) investigate the impact of mix design factors on the fresh and hardened characteristics of geopolymer mortar manufactured from desert dune fines and blast furnace slag. Therefore, Desert sand has outstanding physical and chemical characteristics that differ from pure quartz, clay, and silicate aggregate. When preparing ceramics

Cite this article as: Touil M, Meftah N, Achouri A, Gheriani R, Benessedik R: Mineralogical, physicochemical and thermal investigations of Taibet and Tendla sands material from the Northern Algerian Sahara. Acta Geodyn. Geomater., 20, No. 4 (212), 155–164, 2023. DOI: 10.13168/AGG.2023.0014

with desert sand, the phase transformation and densification take place at low temperatures, while over-sintering is more readily obtained than when using pure quartz and clay. However, desert sand is easier to process into fine powders for ceramic raw materials than pure quartz sand (Shi, 2022). Thus, the physicochemical characteristics of sand are strongly linked to its microstructure, phase composition, phase transition, chemical composition, and particle size. Several investigations have been conducted to assess the physicochemical characterizations of sands to appreciate their potential applications across the world. Amri et al. (2022) investigated the geotechnical and mineralogical features of dune sand-treated clayey soil. They revealed that the treatment significantly improves the mechanical characteristics, particularly for the 30 % dune sand mixture. Hani et al. (2023) and Lazaar et al. (2022) studied the mineralogical and physicochemical properties of Algerian and Tunisian sands respectively, and they successfully extracted an amorphous silica nanoparticle for pollutant dye removal from wastewater. Furthermore, the mineralogical and micromorphological features of Oued Righ region soils from the northeastern Algerian Sahara have been studied by Samia et al. (2023). While, Alawah et al. (2023) researched the physicochemical characterization and genesis of aeolian sand dunes in southern Qatar and the obtained results of Qatari sand dunes were compared to previously published data from Arabian deserts located around the Mediterranean Sea. As well as Pastore et al. (2021) provided a comprehensive provenance study of Sahara Desert sand utilizing a mix of various provenance proxies and state-of-the-art statistical analysis. Zhang et al. (2022) present a critical review of the use of desert sand in the development of sustainable cement-based products. They emphasized the relevance of using desert sand to benefit the economy as well as the environment. Also, Wang et al. (2023) examined the crystallization behavior and characteristics of quartz glass ceramics synthesized from desert sand, in order to synthesizing green and ecologically friendly glass-ceramic materials from abundant sand raw materials. Thus, deeper comprehension of the physicochemical properties of desert (Sahara) sand leads to novel suggestions for using desert sand in various applications.

The Algerian Sahara contains one of the world's largest eolian sand deposits (approximately $2.4.10^6$ km^2). It is crossed by ergs (sand dunes), regs (stony terrain), Ouasis as well as volcanic massifs in the far south. We assume that a good knowledge of the physicochemical properties of these sands and its components can contribute to exploiting this natural resource, in particular for the sustainable applications. Therefore, this research focuses extensive effort on elucidating the microstructure, mineralogy, chemical, and thermogravimetric of two kinks of Algerian Sahara sand (Ouasis sands and dune sands), as standard desert sand and has not been deeply characterized up to now. The purpose of this research is to evaluate the physicochemical and thermal characterizations of Ouasis sands and dune sands in order to assess their applications in various industries as a highly abundant natural source in Algeria.

2. MATERIALS AND METHODS

2.1. SAMPLES PREPARATION

Two distinct locations in the Algerian Sahara were selected to gathered the sand samples. The T1 samples were collected from the dune sands of the Taibet region, a broad region of uninterrupted dunes. However, the T2 samples were collected from the Ouasis sands of the Tendla region. Tendla region is a combination of sandy dunes with scarce vegetation, scattered oases, and salt lakes (Benhaddya et al., 2020). The location and the geographical coordinates of each region are displayed in Figure 1. We gathered around 50 sand samples from various dunes in each location (T1 and T2). The samples were collected from the three sides of each dune, from the top to the bottom, and at different depths for each site. According to Meftah et al. (2021), to get homogeneous samples for each region, we combined the collected samples in equal quantities to generate a final sample that precisely represents the features of each region's sand. To dry the samples and prepare them for analysis, we exposed them to sunlight for three days and ground them before performing a variety of characterization techniques. The sand samples were ground for 15 min using a Retsch Emax grinder machine with a frequency of 800 Hz.

2.2. CHARACTERIZATION METHODS

The particle size distribution of studied sand samples was analyzed using a laser grain size analyzer (LA-960 HORIBA). XRD patterns were obtained using a Bruker model D8 Endeavor Diffractometer that operated at 45 kV and 40mA, λ_{CuK1} =1.5406Å, and a scanning step of 0.02° between 10 and 90°. X'Pert High Score program was used to identify the crystalline phases of our sands. A thermo Scientific Nicolet 380 FT-IR spectrometer operating from 400 to 4000 cm^{-1} was used to identify the characteristic vibrations of chemical bonds found in sand samples. To prepare the samples for this analysis, 2 mg of the powder sand was mixed with 198 mg of dry potassium bromide (KBr), then crushed and pressed with a pressure of 6.10^4 N/cm² for approximately 5 minutes. Scanning electron microscopy with an energy-dispersive X-ray (SEM/ EDX) type Zeiss EVO was used to analyze the morphology and elemental compositions of the sand samples. The chemical composition was examined using an X-ray Fluorescence spectrometer type BRUKER S2 PUMA. To support the previous interpretations, TG/DTA was performed in TA Instruments® equipment, type SDT-Q600 V 20.9 Build 20 for thermal analysis in an inert atmosphere and a temperature reached 1200 °C.

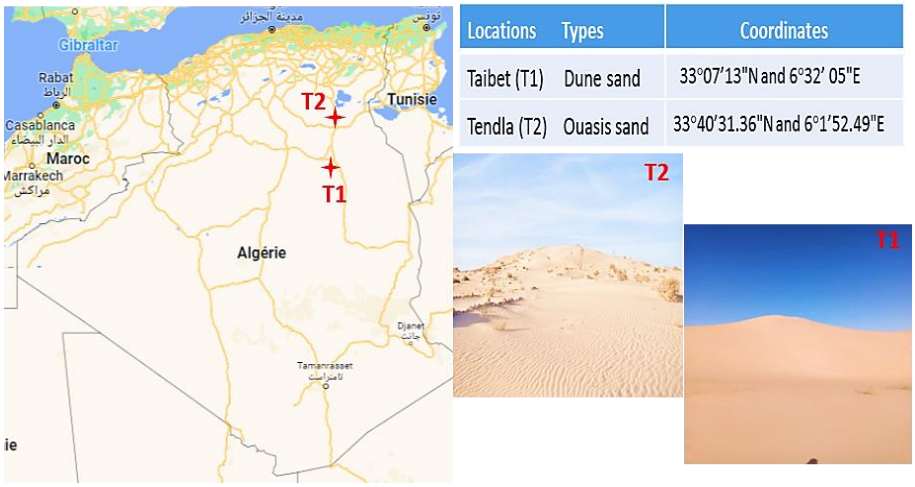

Fig. 1 The location of the two studied areas: Taibet sand (T1) and Tendla sand (T2) and their geographical coordinates.

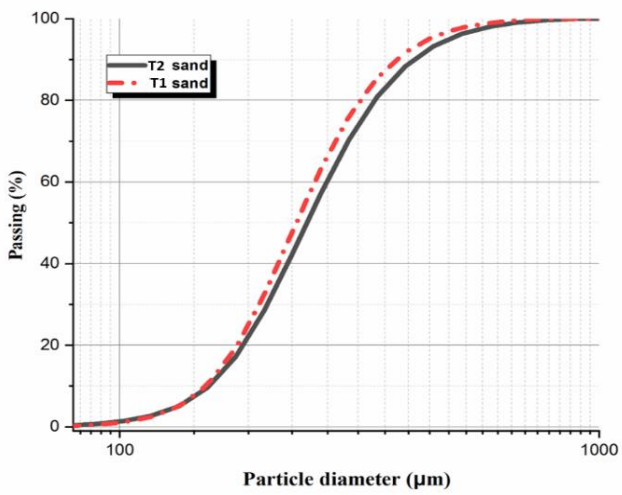

Fig. 2 Particle size distribution of the T1 and T2 sand samples.

3. RESULTS AND DISCUSSION

3.1. GRAIN-SIZE DISTRIBUTION

Particle size distribution can disclose details about the transportation, sorting, and deposition processes of the exanimated sand (Azidane et al., 2021). Figure 2 displays the granulometry distribution of T1 and T2 sand samples. However, the mean grain size (Mz) of T1 and T2 sand was 284 µm and 267 µm, respectively, indicating medium sand grade sands. The sorting (σI) (standard deviation) for T1 and T2 sand samples was 1.473 and 1.432 µm, respectively, indicating moderately well-sorted medium sand. Consequently, these findings demonstrated a good ranking of these sands in the analyzed career and suggested that the sands are deposited in a calm environment with a regular transport agent (Nasri et al., 2021).

However, the Skewness (Ski) was 0.047 µm (positive skewness) for T1 and T2 sand samples, which demonstrates that the sands have a strong symmetry towards the tiny sizes.

3.2. X-RAY DIFFRACTION (XRD) ANALYSIS

The X-ray diffraction spectra may be used to precisely identify the microstructure of T1 and T2 sand samples (Fig. 3). The strong peaks of the diffraction pattern demonstrate that both sand samples have a high crystalline nature. According to the standard pattern JCPDS (N° 46-1045), the diffraction peaks were identified in both sand samples at 2θ° = 20.92, 26.73, 36.61, 42.54, 45.9, 50.26, 54.92, 60.01, 68.39, and 75.74° fit to the α-quartz phase (Meftah et al., 2020).

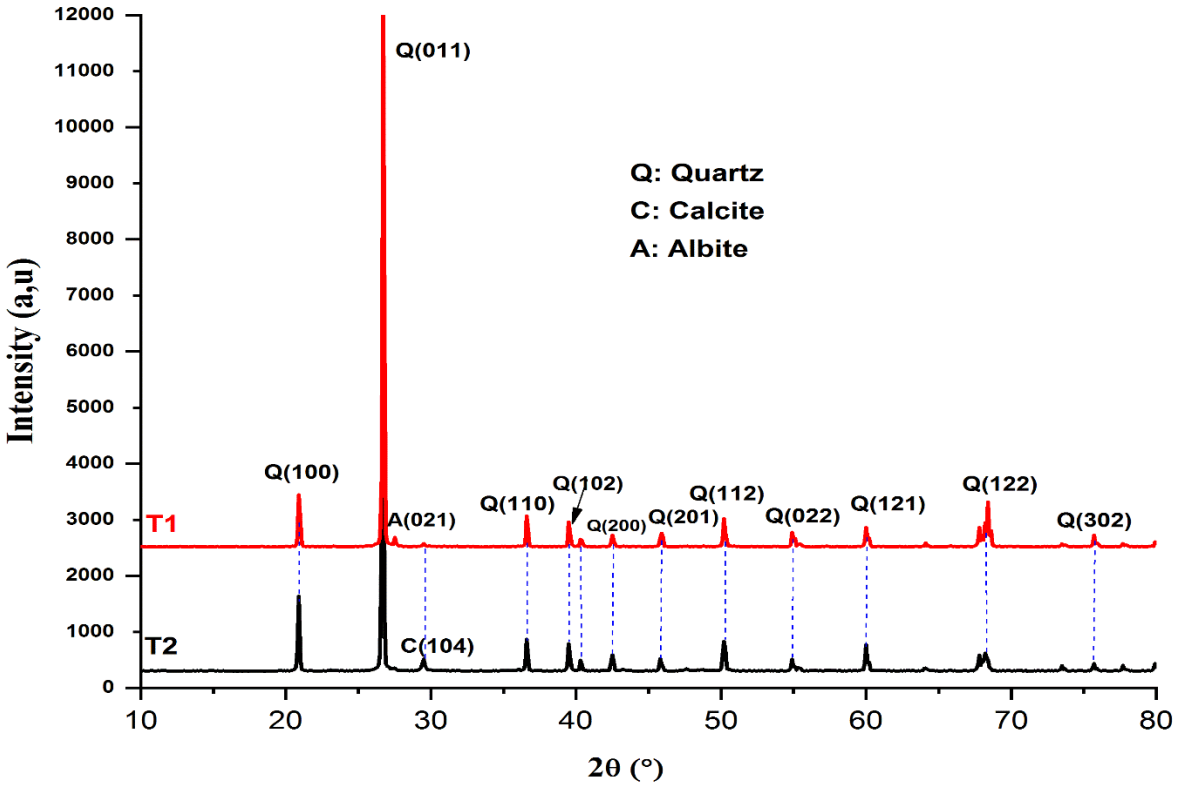

Fig. 3 XRD spectra of T1 and T2 sand samples.

Furthermore, according to the JCPDS (N° 47- 1743), the peaks observed at 29.47° and 47.59° for the T1 and T2 sand samples were generated by calcite (Meftah et al., 2021). Whereas the diffraction peak appears at 27.51° for the T1 sand sample matching Albite mineral (N° 00-041-1480) (Oglesbee et al., 2020). Therefore, the X-ray diffraction results revealed that the T1 dune sand comprises mainly three crystalline phases: α-quartz (SiO_2), Albite ($NaAlSi_3O_8$), and calcite ($CaCO_3$) mineral and the T2 natural sand sample is constituted of two crystalline phases: α-quartz (SiO_2), and Calcite mineral ($CaCO_3$).

The crystallite sizes (D) of quartz in the examined sand were determined from the strong peaks using Scherrer's equation:

$$\boldsymbol{D}(nm) = \frac{0.96\,\lambda}{\beta\,cos\theta} \quad (1)$$

where D is the quartz crystallite size, λ (=1.54 Å) is the used X-rays wavelength, β is the width full of the half maximum (FWHM) in radian of the most intense diffraction peak, and θ is the angle of the most intense peak.

The crystallite sizes of the T1 sand sample was 227 nm, while the crystallite sizes of the T2 sand sample was 136nm; these values are relatively higher than those obtained by Meftah et al. (2020) but remain in the nanometer range, making it of substantial importance to the nanometric industries and nanotechnologies. These findings show that the chemical composition and microstructure vary somewhat depending on the T1 and T2 sand sample location.

3.3. FOURIER-TRANSFORM INFRARED ANALYSIS

This spectroscopy method has the potential to be applied to characterize the fundamental functional groups of its chemical structure units. Figure 4 displays the structure of the main functional groups of the two sand samples (T1 and T2). However, Table 1 summarizes the major functional groups observed in both sands. The functional group distributions of the two types of sand are relatively comparable, while the strongest absorption peaks can be found at 1429, 1083, 792, and 461 cm^{-1}.

The absorption peak at 3444 cm^{-1} observed in T2 sand corresponds to the strong stretching band of the O-H group. While the absorption band identified at 1616 cm^{-1} corresponds to the weak O–H bending mode of adsorbed water which could have been attached to the silica surface (Nasri et al., 2021).

The major peaks were seen in both sand samples at 876 cm^{-1}, 1083 cm^{-1}, and 1879cm^{-1} corroborate the Si–O–Si symmetric bending and stretching vibration, respectively. However, the absorption band appears in T1 and T2 samples at 461cm^{-1} indicating Si–O–Si asymmetrical bending vibration (Chandrasekaran et al., 2021). The common absorption band at 694, 777, and 793 cm^{-1} present Si–O symmetrical bending and

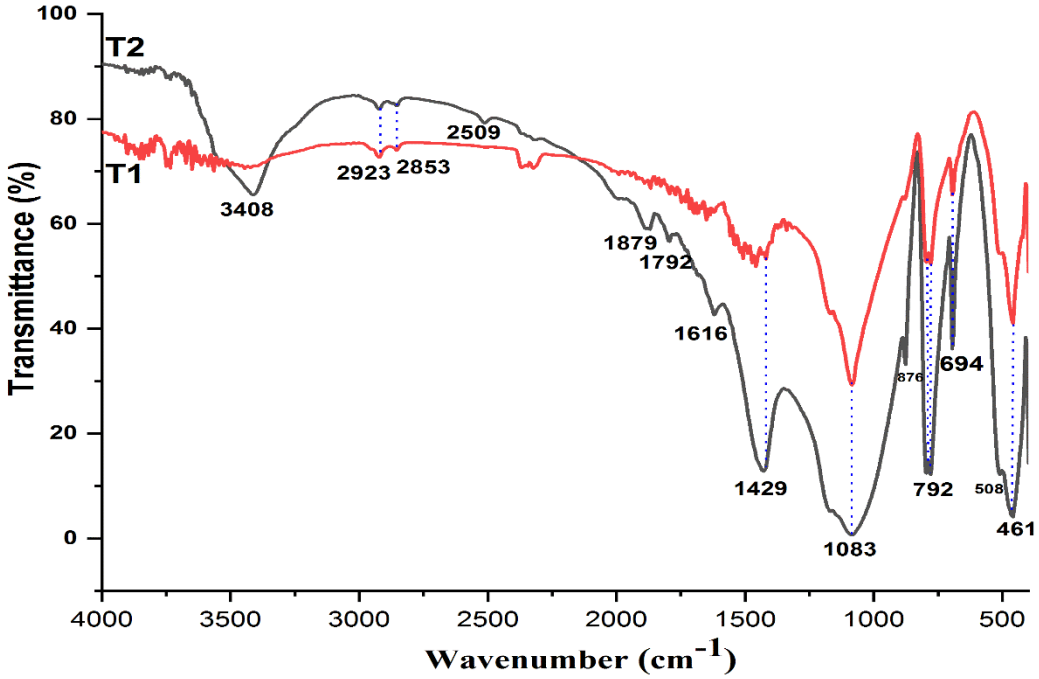

Fig. 4 FTIR spectra of T1 and T2 sand samples.

Table 1 The main absorption bands and associated minerals for T1 and T2 sand samples.

Band (cm^{-1})		Bond (vibration mode)	Compound
T1 sample	T2 sample		
461	461	Si–O–Si asymmetrical bending vibration	Quartz
508	508	Si–O–Al asymmetrical bending vibration	Quartz
694	694	Si–O symmetrical bending	Quartz
777	777	Si–O symmetrical stretching	Quartz
793	793	Si–O symmetrical stretching	Quartz
876	876	Si–O–Si symmetrical bending	Quartz
1083	1083	Si–O–Si symmetrical stretching	Quartz
1429	1429	$(CO_3)^{-2}$ asymmetrical and symmetrical stretching	Calcite
-	1616	H–OH bending	Water
-	1792	$(CO_3)^{-2}$ plane bending and symmetrical stretching combination mode	Calcite
-	1879	Si–O–Si Stretching vibration	Quartz
-	2509	$(CO_3)^{-2}$ asymmetrical and symmetrical stretching vibration	Calcite
2853	2853	C–H stretching vibration	Organic carbon
2923	2923	C–H stretching vibration	Organic carbon
-	3408	H–O–H stretching vibration	Water

stretching respectively. Whereas, the IR absorption band at 508 cm^{-1} indicates a Si–O–Al asymmetrical bending vibration. These characteristic FTIR peaks confirm the existence of quartz as a main component in T1 and T2 sand samples. The existence of double absorption peaks at 792 and 777 cm^{-1} indicates the presence of quartz in α-phase in both samples (Beddiaf et al., 2015). The FTIR spectrum of the T2 sand sample showed a weak peak at 1792 and 2509 cm^{-1} which may be attributed to the $(CO_3)^{-2}$ plane bending and the symmetrical stretching combination mode of $CaCO_3$. Furthermore, an absorption peak observed at 1429 cm^{-1} in T1 and T2 samples could correspond to $(CO_3)^{-2}$ asymmetrical and symmetrical stretching vibration in calcite minerals. The absorption peaks found at around 2853 and 2923 cm^{-1} were related to the C–H stretching vibration which may correspond to organic matter subsisting in the sand samples.

Table 2 The chemical compositions of T1 and T2 sand samples.

	SiO_2	$Al2O_3$	Fe_2O_3	CaO	MgO	K_2O	Na_2O	SO_3	PAF
T1 sand	95.34	0.79	0.41	0.93	0.12	0.49	0.04	0.06	2.50
T2 sand	90.09	0.67	0.33	3.48	0.16	0.43	0.03	0.65	4.23

Table 3 The geochemistry results of the T1 and T2 sand sample

Sample	CMI (=SiO_2/Al_2O_3)	Fe_2O_3 + MgO (%)	Al_2O_3/SiO_2	Al_2O_3 + Na_2O + K_2O (%)	CIA	CIW
T1	120.68	0.53	0.0083	1.32	35.11	44.89
T2	134.46	0.49	0.0074	1.13	14.53	16.03

Therefore, the FT-IR spectrum demonstrates that the T1 and T2 sand samples are mainly composed of α- quartz (SiO_2) and lower content of calcite ($CaCO_3$) mineral, nevertheless T1 sand contains a trace quantity of calcite. The FTIR study results are in good agreement with the XRD analysis.

The crystallinity index of quartz (*CIQ*) in the studied samples is calculated following the equation (2) (Hlavay et al., 1978):

$$CIQ = \frac{A_{795}}{A_{779}} \quad (2)$$

where A_α is the absorbance at wavenumber α, and this was determined as follows:

$$A_\alpha = log\left(\frac{T_{0\alpha}}{T_\alpha}\right) \quad (3)$$

where T_α is the transmittance value at wavenumber α.

The degree of crystallinity of quartz (*ICQ*) was determined to be 0.65 for the T1 sample and 0.85 for the T2 sample. Because the crystallinity index is inversely related to material crystallinity (Suresh et al., 2011), the computed ratio suggests that T1 sand quartz has higher crystallinity than T2 sand quartz.

3.4. CHEMICAL ANALYSIS

The chemical compositions of the T1 and T2 sand sample determined by XRF analyses are summarized in Table 2. Silica (SiO_2) is the most abundant oxide in both sand samples, accounting for 95 % in the T1 and 90 % in the T2 samples. Furthermore, the T2 sand sample has more calcium oxide (CaO) amounts than the T1 sand sample, with 3.4 % in the T2 sample and 0.93 % in the T1 sand sample. In addition, very low ratios of other oxides like Aluminum oxide, Iron oxide, Magnesium oxide, Potassium oxide, Sodium oxide, and Sulphur oxides have been identified in both samples. Therefore, the high silica concentration of both sand samples ensures their siliceous origin and represents the studied sand's quartz-rich character. However, the very low concentrations of these oxides in the T1 sand sample suggest the higher purity of quartz in this sample.

Based on XRF findings, the geochemistry analysis of T1 and T2 are determined and summarized in the Table 3. The geochemistry study can reveal information about the provenance of the samples, as well as weathering conditions. The chemical maturity index (*CMI*) defined as the ratio between SiO_2 and Al_2O_3. Also, the chemical index of alteration (*CIA*) was computed as [Al_2O_3×100/(Al_2O_3 + Na_2O+ CaO + K_2O)] and the chemical index of weathering (*CIW*) is computed as [Al_2O_3 × 100/(Al_2O_3 + CaO + Na_2O)] (Meftah et al., 2021).

These parameters are widely used indexes for determining the degree and duration of weathering in deposits. According to Table 3, the chemical maturity index (*CMI*) of T1 sand is around 121 and 134 for T2 sand samples, indicating the high chemical maturity of the examined samples.

Furthermore, based on the binary variation diagram of SiO_2 versus Al_2O_3+K_2O+Na_2O, the examined sand samples developed under semi-humid circumstances. In addition, T1 and T2 sand samples involve Fe_2O_3+ MgO<0.8 % and Al_2O_3/SiO_2<0.3, indicating that they are associated with passive continental margins, according to the Bhatia's (1983) tectonic model (Bhatia, 1983). Moreover, the *CAI* and *CIW* ratios of the T1 and T2 sand samples indicate a low degree of chemical weathering and environmental conditions (Fedo et al., 1995).

3.5. MORPHOLOGICAL AND ELEMENTAL COMPOSITIONS ANALYSIS

The morphology of granular materials, such as sands, is important because grain shape influences their physical, mechanical, and hydraulic properties. Backscattered electron (BSE) micrographs and EDX results of the examined sand samples acquired by scanning electron microscopy are shown in Figure 5. T1 and T2 sand grains have rounded, sub-rounded, flat elongated, angular, and subangular shapes, while T1 sand has also some smooth rounded grains.

This feature can be caused by long-distance water transportation, which allows for more interactions and collisions between grains, resulting in higher abrasion and smoother surfaces (Wolfe et al., 2023). Continuous tumbling and rolling during transportation smooth down inconsistencies and sharp edges. Moreover, T2 sand grains are larger in size than the T1 sand grains.

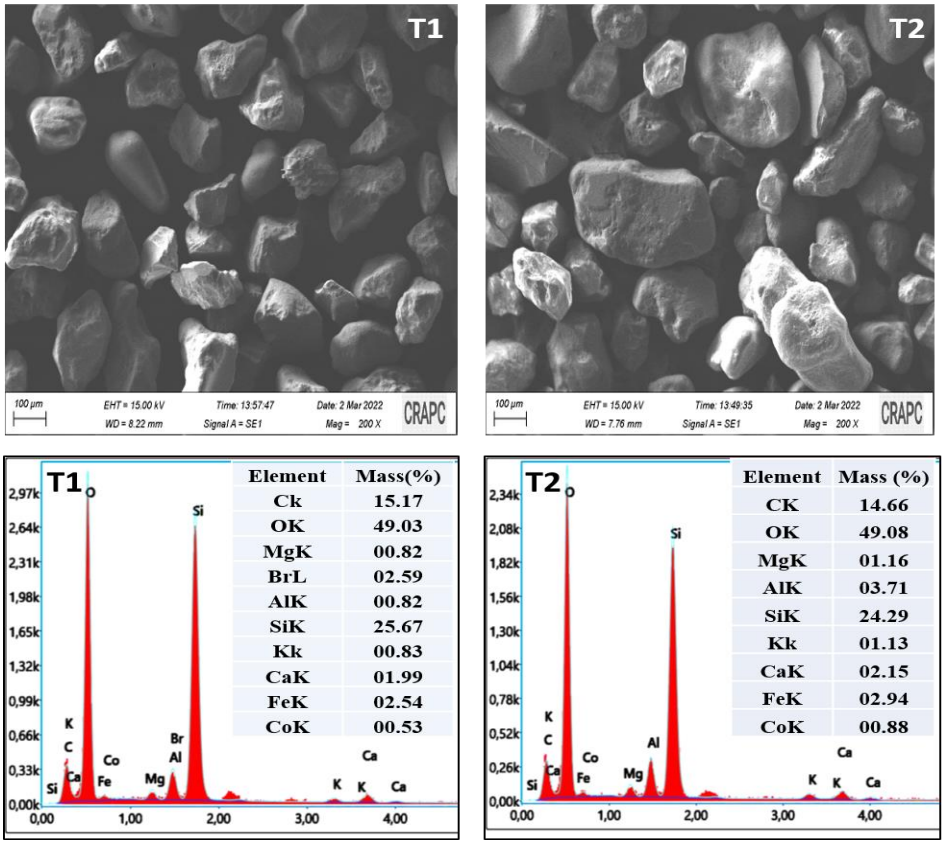

Fig. 5 SEM/EDX analysis of T1 and T2 sand.

Figure 5 shows that EDX analysis revealed that Si and O are the most abundant elements in both T1 and T2 samples. The Si peak, on the other hand, was more intense in the T1 sand sample, indicating that quartz was more abundant in this sand sample. Furthermore, the EDX spectra show the presence of contaminants in both samples at varying rates, such as Al, Mg, Ca, Fe, K, and Co.

3.6. THERMAL ANALYSIS

Thermogravimetric and differential thermal analysis ((TGA/DTA) of T1 sand and T2 sand were illustrated in Figure 6. The TG plot for the T1 sand sample shows a first weight loss (around 1.15 %) between 25 and 548 °C, followed by a second mass loss (about 0.83 %) from 548 °C to 679 °C. While the T2 sand sample exhibits three stages of weight loss: the first (roughly 0.64 %) occurs between room temperature and 540 °C, the second (around 2.73 %) occurs between 540 °C and 732 °C, and the final (about 0.64 %) occurs between 997 °C and 1160 °C. Thus, the overall mass loss was 1.98 % against 4.01 % for the T2 sand sample (Fig. 5). The mass loss seen between ambient and 500 °C reflects the elimination of physically and chemically bonded water (Alshaaer et al., 2021). Additionally, oxidation of potential organic materials may occur between 200 and 400 °C (Mikhailova et al., 2022). The weight loss noticed between 530 and 740 °C was strongly linked to the calcium carbonate concentration (Meftah et al., 2023), which exceeded 0.8 % for the T1 sand sample and 2.7 % for the T2 sample. The DTA spectrum of both sand samples shows three endothermic peaks at 105, 574, and 700 °C, as well as one exothermic peak at 886 °C for T2 sand and 1014 °C appear for T1 sand. The endothermic peak positioned at 68.9 °C was attributed to the loss of water absorbed on the sand surface. Further, the endothermal peaks at 572 °C and 700 °C were assigned to transformations of α-quartz to β-quartz and β-quartz to β-tridymite, respectively (Shi et al., 2023). At 886 and 1014 °C, we can see an exothermic peak generated by the crystallization (Luo et al., 2023).

The thermogravimetric and differential thermal analysis confirm the XRD and FTIR findings and prove that calcite is most abundant in T2 sand and consequently, T1 quartz has higher purity than the T2 sample.

3.7. POTENTIALITIES OF USE

According to the international standards, the potential applications of the investigated sand samples mainly depend on three major selection criteria including grain size distribution, chemical compositions, and mineralogical criteria (Meftah et al., 2021; Osseni et al., 2018 and Platias et al., 2014). The comparison of the physicochemical characteristics of Tendla and Taibet sands with criteria

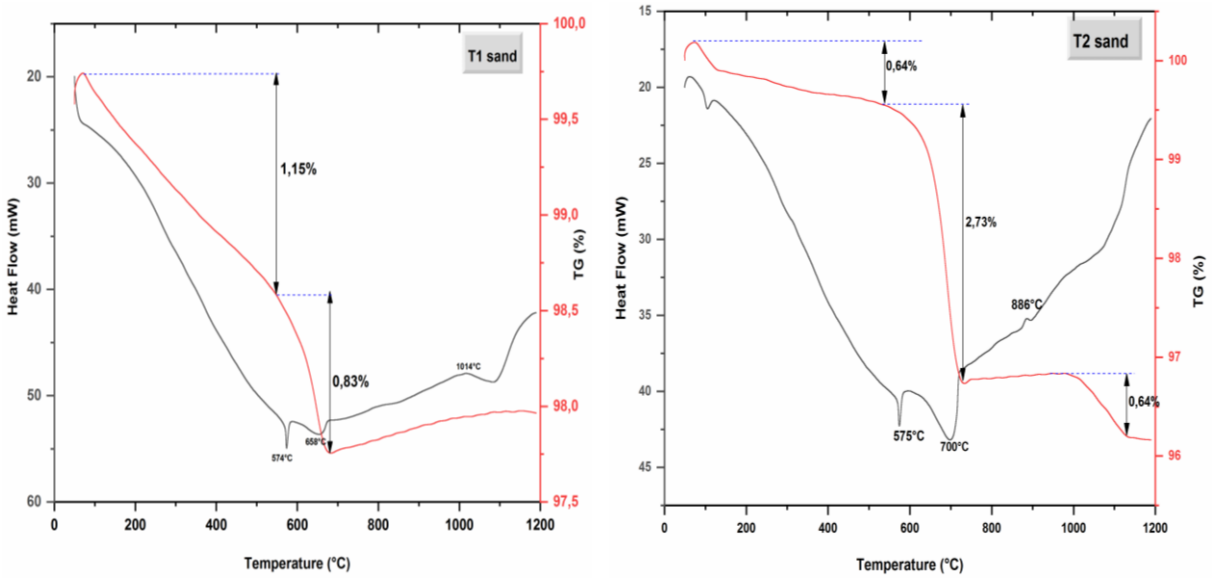

Fig. 6 Thermal analysis curves (DTA-GTA) of T1 and T2 sand powders.

for the use of sands revealed their possible utilization in various civil engineering applications such as foundry, Bricks, fillers, aggregate in ceramic, concrete, and mortar. However, the examined sand grains are promising candidates for solar energy storage, particularly as solar distillers (Meftah et al., 2021). Whereas, the potential use of Tendla and Taibet sands for glass industry and photovoltaic applications needs additional treatment to remove harmful impurities.

4. CONCLUSION

The growing exploitation of silicate inorganic materials and decreasing mineral resources necessitates the use of dune sand as a raw resource for silicate materials. This study conducted an intensive investigation of the physicochemical characteristics of Algerian Sahara-sand-based materials in order to accomplish the objective of sustainable development. The particle size, microstructure, chemical composition, and the phase composition of Sahara sands were little affected by the sample location in the Sahara. The granulometric distribution indicated that the studied sand is moderately well-sorted medium sand. The XRD examination reveals that alpha-quartz dominates the Sahara sand, with only low amounts of calcite and Albite. The crystallite size of sand quartz ranged from 136-227 nm, demonstrating the nanometric aspect of desert sand quartz. Furthermore, the chemical analysis confirms that the desert sands mainly consist of about 90-97.63 % of SiO_2, minor CaO mineral (about 0.93-3.48 %), as well as minimal amounts of other oxides (Al_2O_3, Fe_2O_3, Na_2O, MgO). The quartz crystallinity has been determined to be 0.65-0.85, confirming the high crystalline structure of quartz. As well as Sahara sand grains presented a variety of shape and microstructure. These physicochemical properties demonstrated that these sands may be exploited in a wide range of engineering applications, including construction, foundry, ceramic industry, solar energy storage, and glass production.

ACKNOWLEDGEMENTS

The authors are deeply grateful to the staff of the Renewable Energy Development Unit in Arid Zones (UDERZA) from El-Oued University, the staff of the Center for Scientific and Technical Research in Physicochemical Analysis (CRAPC) of Laghouat, Bedjaia, and Ouargla; as well as to the Laboratory of Radiation and Plasmas and Surface Physics (LRPPS); the Physics and the Chemistry Department at the Ouargla University - Algeria.

DECLARATIONS

Competing Interests: The authors have no conflicts of interest to declare that are relevant to the content of this article.

Funding: No funds, grants, or other support was received.

Author Contributions: All authors contributed to the study conception and design. Material preparation, data collection and analysis were performed by Meriem Touil and Nassima Meftah. The first draft of the manuscript was written by Nassima Meftah and all authors commented on previous versions of the manuscript. All authors read and approved the final manuscript

REFERENCES

Al-Awah, H. and Matter, W.S.: 2023, Physicochemical characterization and origin of aeolian sand dunes in Southeastern Qatar: A comparative study with Mediterranean sand dunes. Adv. Geosci., 63, 1–13. DOI: 10.5194/adgeo-63-1-2023

Alshaaer, M.: 2021, Microstructural characteristics and long-term stability of wollastonite-based chemically bonded phosphate ceramics. Int. J. Appl. Ceram. Technol., 18, 2, 319–331. DOI: 10.1111/ijac.13661

Amri, S., Akchiche, M., Bennabi, A. and Hamzaoui, R.: 2019, Geotechnical and mineralogical properties of treated clayey soil with dune sand. J. Afr. Earth Sci., 152, 140–150. DOI: 10.1016/j.jafrearsci.2019.01.010

Atta, A.M., Abdullah, M.M., Al-Lohedan, H.A. and Mohamed, N.H.: 2019, Coating sand with new hydrophobic and superhydrophobic silica/paraffin wax nanocapsules for desert water storage and transportation. Coatings, 9, 2, 124. DOI: 10.3390/coatings9020124

Azidane, H., Michel, B., Bouhaddioui, M.E., Haddout, S., Magrane, B. and Benmohammad, A.: 2021, Grain size analysis and characterization of sedimentary environment along the Atlantic Coast, Kenitra (Morocco). Mar. Georesources Geotechnol., 39, 5, 569–576. DOI: 10.1080/1064119X.2020.1726536

Beddiaf, S., Chihi, S. and Leghrieb, Y.: 2015, The determination of some crystallographic parameters of quartz, in the sand dunes of Ouargla, Algeria. J. Afr. Earth Sci., 106, 129–133. DOI: 10.1016/j.jafrearsci.2015.03.014

Benhaddya, M.L., Halis, Y. and Hamdi-Aïssa, B.: 2020, Assessment of heavy metals pollution in surface and groundwater systems in Oued Righ region (Algeria) using pollution indices and multivariate statistical techniques. Afr. J. Aquat. Sci., 45, 3, 269–284. DOI: 10.2989/16085914.2019.1703635

Bhatia, M.R.: 1983, Plate tectonics and geochemical composition of sandstones. J. Geol., 91, 6, 611–627. DOI: 10.1086/628815

Chandrasekaran, A., Senthil Kumar, C.K., Sathish, V., Manigandan, S. and Tamilarasi, A.: 2021, Effect of minerals and heavy metals in sand samples of Ponnai river, Tamil Nadu, India. Sci. Rep., 11,1, 23199. DOI: 10.1038/s41598-021-02717-x

El-Mir, A., El-Hassan, H., El-Dieb, A. and Alsallamin, A.: 2022, Development and optimization of geopolymers made with desert dune sand and blast furnace slag. Sustainability, 14, 13, 7845. DOI: 10.3390/su14137845

Fattouh, M.S., Tayeh, B.A., Agwa, I.S. and Elsayed, E.K.: 2023, Improvement in the flexural behavior of road pavement slab concrete containing steel fibre and silica fume. Case Stud. Constr. Mater., 18, e01720. DOI: 10.1016/j.cscm.2022.e01720

Fedo, C.M., Nesbitt, H.W. and Young, G.M.: 1995, Unravelling the effects of potassium metasomatism in sedimentary rocks and paleosols, with implications for paleoweathering conditions and provenance. Geology, 23, 921–924. DOI: 10.1130/0091-7613

Hani, A., Meftah, N., Zeghoud, L., Sdiri, A. and Jawad, H.A.: 2023, Statistical optimization and desirability function for producing nano silica from dune sand by sol–gel method towards methylene blue dye removal. J. Inorg. Organomet. Polym. Mater., 1–16. DOI: 10.1007/s10904-023-02612-0

Hlavay, J., Jonas, K., Elek, S. and Inczedy, J.: 1978, Characterization of the particle size and the crystallinity of certain minerals by IR spectrophotometry and other instrumental methods- II. Investigations on quartz and feldspar. Clays Clay Miner., 26, 2, 139–143. DOI: 10.1346/CCMN.1978.0260209

Karnati, S.R., Agbo, P. and Zhang, L.: 2020, Applications of silica nanoparticles in glass/carbon fiber-reinforced epoxy nanocomposite. Compos. Commun., 17, 32–41. DOI: 10.1016/j.coco.2019.11.003

Koçak, B., Fernandez, A.I. and Paksoy, H.: 2020, Review on sensible thermal energy storage for industrial solar applications and sustainability aspects. Sol. Energy, 209, 135–169. DOI: 10.1016/j.solener.2020.08.081

Lazaar, K., Pullar, R., Hajjaji, W., Mefteh, S., Medhioub, M. and Jamoussi, F.: 2022, Preparation of silica gel obtained from early cretaceous Sidi Aich Sands (Central Tunisia) and its potential to remove Pollutant Dye Anionic from Wastwaters. Silicon, 1–12. DOI: 10.1007/ s12633-021-01251-9

Liu, Y., Li, Y. and Jiang, G.: 2020, Orthogonal experiment on performance of mortar made with dune sand. Constr. Build. Mater., 264, 120254. DOI: 10.1016/j.conbuildmat.2020.120254

López-Cuevas, J., Interial-Orejón, E., Gutiérrez-Chavarría, C.A. and Rendón-Ángeles, J.C.: 2017, Synthesis and characterization of cordierite, mullite and cordierite-mullite ceramic materials using coal fly ash as raw material. MRS Adv., 2, 62, 3865–3872. DOI: 10.1557/adv.2018.3

Luo, H., Shi, Z.M., Wang, H. and Wang, W.: 2023, The microstructure, phase transformation and sinterability of desert sand. Mater. Today Commun., 35, 105685. DOI: 10.1016/j.mtcomm.2023.105685

Meftah, N. and Mahboub, M. S.: 2020, Spectroscopic characterizations of sand dunes minerals of El-Oued (Northeast Algerian Sahara) by FTIR, XRF and XRD analyses. Silicon, 12, 1, 147–153. DOI: 10.1007/s12633-019-00109-5

Meftah, N., Hani, A., Merdas, A., Sadik, C. and Sdiri, A.: 2021, A holistic approach towards characterizing the El-Oued siliceous sand (eastern Algeria) for potential industrial applications. Arab. J. Geosci., 14, 1–14. DOI: 10.1007/s12517-021-08591-1

Meftah, N. and Hani, A.: 2022, Characterization of Algerian dune sand as a source to metallurgical-grade silicon production. Mater. Today Proc., 51, 2105–2108. DOI: 10.1016/j.matpr.2021.12.366

Meftah, N., Hani, A. and Merdas, A.: 2023, Extraction and physicochemical characterization of highly-pure amorphous silica nanoparticles from locally available dunes sand. Chem. Afr., 1–10. DOI: 10.1007/s42250-023-00688-2

Mikhailova, A.N., Kayukova, G.P., Varfolomeev, M.A. and Emelyanov, D.A.: 2022, Thermogravimetric parameters of the oxidation of organic matter and asphaltenes from the rocks of the Permian deposits of heavy oil field before and after catalytic hydrothermal treatment. Fuel, 313, 122641. DOI: 10.1016/j.fuel.2021.12264

Nasri, H., Kermani, S., Abbassi, M.A. and Omri, A.: 2021, Characterization of sand from Jebel Ad-Darin Sened (Gafsa-Tunisia). Silicon, 13, 11, 3827–3834. DOI: 10.1007/s12633-020-00687-9

Oglesbee, T., McLeod, C.L., Chappell, C. et al.: 2020, A mineralogical and geochemical investigation of modern aeolian sands near Tonopah, Nevada: sources and environmental implications. Catena, 194, 104640. DOI: 10.1016/j.catena. 2020.104640

Osseni, S.A., Masseguin, M., Sagbo, E.V., Neumeyer, D., Kinlehounme, J.Y., Verelst, M. and Mauricot, R.: 2019, Physico-chemical characterization of siliceous sands from Houéyogbé in Benin Republic (West Africa): potentialities of use in glass industry. Silicon, 11, 2015–2023. DOI: 10.1007/s12633-018-0022-y

Pastore, G., Baird, T., Vermeesch, P., Bristow, C., Resentini, A. and Garzanti, E.: 2023, Provenance and recycling of Sahara Desert sand. Earth. Sci. Rev., 216, 103606. DOI: 10.1016/j.earscirev.2021.103606

Radwan, O.A., Humphrey, J.D., Hakeem, A.S. and Zeama, M.: 2021, Evaluating properties of Arabian desert sands for use in solar thermal technologies. Sol. Energy Mater. Sol. Cells, 231, 111335. DOI: 10.1016/j.solmat.2021.111335

Smaida, A., Haddadi, S. and Nechnech, A.: 2019, Improvement of the mechanical performance of dune sand for using in flexible pavements. Constr. Build. Mater., 208, 464–471. DOI: 10.1016/j.conbuildmat.2019.03.041

Shapakidze, E., Gejadze, I., Nadirashvili, M., Maisuradze, V., Petriashvili, T. and Skhvitaridze, A.: 2019, Using clay rocks of Georgia to obtain high-active Pozzolanic Additives to Portland Cement. Int. J. Appl. Eng. Res., 14, 18, 3689–3695.

Shi, Z.: 2022, Green manufacturing of silicate materials using desert sand as a raw-material resource. Constr. Build. Mater., 338, 127539. DOI: 10.1016/j.conbuildmat.2022.127539

Shi, Z., Zhang, Y., Luo, W., Liu, Z. and Wang, W.: 2023, Substitution of desert sand for pure quartz to improve phase transformation and densification of SiO_2-ZrO_2 composite ceramics. Available at SSRN, 4511645. DOI: 10.2139/ssrn.4511645

Suresh, G., Ramasamy, V. and Ponnusamy, V.: 2011, Mineralogical and thermoluminescence characterizations of the river sediments from Tamilnadu, India. Nat. Resour. Res., 20, 4, 389–399. DOI: 10.1007/s11053-011-9158-9

Ter Teo, P., Anasyida, A.S., Kho, C.M. and Nurulakmal, M.S.: 2019, Recycling of Malaysia's EAF steel slag waste as novel fluxing agent in green ceramic tile production: Sintering mechanism and leaching assessment. J. Clean. Prod., 241, 118144. DOI: 10.1016/j.jclepro.2019.118144

Wang, W., Song, J., Shi, Z., Sun, W. and Xue, L.: 2023, Crystallization behavior and properties of quartz glass-ceramics synthesized from desert sand. Ceram. Int. DOI: 10.1016/j.ceramint.2023.10.111

Wolfe, S.A., Demitroff, M., Neudorf, C.M., Woronko, B., Chmielowska-Michalak, D. and Lian, O.B.: 2023, Late Quaternary eolian dune-field mobilization and stabilization near the Laurentide Ice Sheet limit, New Jersey Pine Barrens, eastern USA. Aeolian Res., 62, 100877.

Zhang, M., Zhu, X., Shi, J., Liu, B., He, Z. and Liang, C.: 2022, Utilization of desert sand in the production of sustainable cement-based materials: A critical review. Constr. Build. Mater., 327, 127014. DOI: 10.1016/j.conbuildmat.2022.127014